UPPSALA
UNIVERSITET

Phase diagrams of finite spin chains with coupled spin and lattice vibrations

Siri A. Berge

Degree Project C in Physics, 15hp

Supervisor: Jonas Fransson
Subject reader: Anders Bergman
Examinator: Matthias Weiszflog

July 14, 2021

Abstract

The spin-lattice coupling is due to itinerant electrons interacting with both spins of ions and phonons, mediating a coupling between magnetic spin moments and lattice vibrations. In this project, the coupling is studied systematically for finite quantum spin chains of size 2 – 10. The coupling is included in a Hamiltonian model with the Heisenberg exchange interaction and an external magnetic field resulting in an eigenvalue problem which is solved numerically to find phase diagrams of the magnetic moment of the system depending on an external magnetic field and the lattice vibration parameter α. The eigenvalue problem is also solved analytically for the 2-ion chain, dimer, and 3-ion chain, trimer, systems. Based on these phase diagrams two propositions are made: the effect of the coupling is larger than an external magnetic field and the behavior of the coupling converges to a common phase diagram for larger spin chains.

Sammanfattning

Kopplade spinn- och vibrationsfrihetersgrader beror på kringvandrande elektroner som växelverkar med både spin och fononer, vilket förmedlar en koppling mellan magnetiskt spinmoment och gittervibrationer. I detta projekt studeras denna koppling systematiskt för ändliga spin-kedjor av 2–10 joner. Systemet beskrivs av en Hamiltonian med Heisenberg modellen som beskriver spin-spin kopplingen samt ett externt magnetiskt fält. Detta egenvärdesproblem löses analytiskt för dimer- och trimersystem samt numeriskt för längre kedjor. Lösningarna används för att ta fram fasdiagram av de magnetiska momenten av kedjorna beroende på externt magnetfält och spin- och vibrationsfrihetsgradsparametern α. Baserat på dessa fasdiagram, framförs två propositioner: kopplingens effekt är större än ett externt magnetfält och kopplingens beteende konvergerar till ett enhetligt fasdiagram för större spinnkedjor.

Contents

1 Introduction

Magnetism is a fundamental part of society today, from refrigerators to cars to computers. It is important to understand and study the fundamental properties of magnetism to continue to be able to discover, explore, and understand novel materials and their properties.

A relatively obscure and unknown part of magnetism is the relationship between the individual magnetic moments, a result of spins, in the material and the mechanical vibrations of the positions of the spins, i.e. lattice vibrations. This is governed by the spin-lattice coupling, which is the subject of this work. Fundamental understanding of the spin-lattice coupling is important for many reasons and there are many future applications including the emerging field of spintronics and magnonics (devices working on the principles of spin waves and magnetism) ([1], [2]).

One recent example of a project making use of the phenomenon of the spin-lattice coupling is an experiment which proved that sound waves can generate coherent spin waves (spin waves are a collective excitation of spins) [3]. While this experiment does not discuss the coupling, the result implies that this coupling exists and can be used with great effect.

The spin-lattice coupling behavior might also be a factor in temperature activated ferromagnetism. Recently published results show experimentally that some ferromagnets become more ferromagnetic at higher temperatures, which goes against previously known results ([4], [5]).

The purpose of this work is to systematically observe and describe the effect of the spin-lattice coupling on a finite spin chain. The simplest cases, that of the dimer with two interacting spins and trimer with three, are studied both analytically and numerically, whilst higher order systems are studied exclusively numerically.

2 Theory

2.1 Magnetism

Magnetism in materials is a quantum mechanical phenomenon. Due to an unpaired electron, an atom will have a spin magnetic moment, and if these moments are aligned the material will have a non-zero magnetization. The magnetic moment orientations may be influenced by an applied magnetic field. In the case of diamagnetism, the moments will orient to counteract the imposed field and in paramagnetic materials the moments will align with the applied field. Ferro- and antiferromagnetic materials exhibit a property called spontaneous magnetization, where the moments may align without an imposed field when below a critical temperature. This is also called ordered magnetism and is due to the exchange interaction. Ferromagnetic materials are strongly magnetic with all spins aligned, whereas antiferromagnetic materials have pairwise oppositely aligned spins and thus has no net magnetization [6].

2.2 Heisenberg Hamiltonian

A useful model of ferromagnetism is the Heisenberg Hamiltonian, which is used to describe the exchange interaction between localized electron spins ([7],[6]). The model is best realized in materials which are magnetic insulators with localized magnetic moments due to unfilled electron shells [8]. However, the model is useful to describe general magnetic phenomena [9].

The Heisenberg Hamiltonian is defined as follows:

$$\mathcal{H} = -\sum_{ij} J_{i,j} \mathbf{S}_i \cdot \mathbf{S}_j \tag{1}$$

with spin operators $\mathbf{S}_{i,j}$ and exchange constant $J_{i,j}$. The indices i represent ion positions and j are the adjacent ion, see Figure 1. In this work, these are spin 1/2 particles, such as electrons, and the spin operators are $\mathbf{S}_{x,y,z} = \sigma_{x,y,z}/2$ with Pauli matrices $\sigma_{x,y,z}$. The exchange constant $J_{i,j}$ describes the interaction between the spins and can be used to model different types of magnetism. For antiferromagnetism, a negative exchange coupling is used since this returns an antiferromagnetic state as its minimum energy state. For ferromagnetism a positive constant is used analogously.

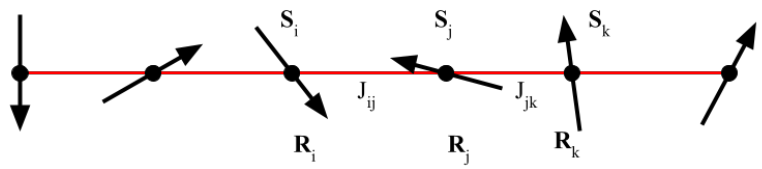

Figure 1: Linear Heisenberg spin chain with exchange coupling J_{ij}, spin operators $\mathbf{S}_i$, and lattice sites $\mathbf{R}_i$.

In this study, the exchange coupling is assumed to be equal between each consecutive lattice site and zero for any site further than nearest neighbor. This

can be assumed since the exchange is due to electrons and should decrease with inverse radius in a linear system.

The Heisenberg Hamiltonian can then be found for general N-size systems using the dimer Hamiltonian and projecting this on longer spin chains. For a dimer the Hamiltonian is

$$\begin{aligned}
\mathcal{H}_2 &= -J\mathbf{S}_1 \cdot \mathbf{S}_2 && \text{(2a)}\\
&= -J(S_1^x S_2^x + S_1^y S_2^y + S_1^z S_2^z) && \text{(2b)}\\
&= -J/4(\sigma_1^x \otimes \sigma_2^x + \sigma_1^y \otimes \sigma_2^y + \sigma_1^z \otimes \sigma_2^z) && \text{(2c)}\\
&= -J/4 \begin{pmatrix} 1 & 0 & 0 & 0 \\ 0 & -1 & 2 & 0 \\ 0 & 2 & -1 & 0 \\ 0 & 0 & 0 & 1 \end{pmatrix} && \text{(2d)}
\end{aligned}$$

and the basis of the dimer Hamiltonian is

$$\begin{pmatrix} |\uparrow\uparrow\rangle \\ |\uparrow\downarrow\rangle \\ |\downarrow\uparrow\rangle \\ |\downarrow\downarrow\rangle \end{pmatrix}. \tag{3}$$

For the trimer, the dimer Hamiltonian is projected as follows

$$\mathcal{H}_3 = \mathcal{H}_2 \otimes \sigma^0 + \sigma^0 \otimes \mathcal{H}_2 \tag{4}$$

where σ^0 is the 2x2 identity. By induction, it is seen that for a system of N interacting spins, the Hamiltonian is then given by

$$\mathcal{H}_{N+1} = \mathcal{H}_N \otimes \sigma^0 + \sigma^0 \otimes \mathcal{H}_N. \tag{5}$$

2.3 Zeeman term

An applied external homogeneous magnetic field can be included in the model which breaks the rotational symmetry of the Heisenberg Hamiltonian [8]. The term describing the field is called the Zeeman term. This term is included since an external field is easily controlled in an experimental setting. The direction of the magnetic field is chosen to be the z-direction. Here the parameter $B_0 = g\mu_B B$, where g is the g-factor which is equal to 2 for pure spin moments, $\mu_B \approx 5.8 * 10^{-5}$ eVT^{-1} is the Bohr magneton, and B is an applied magnetic field in Tesla. B_0 thus has the units eV.

$$\mathcal{H}_{\text{Zeeman}} = B_0 \sum_i \mathbf{S}_i \tag{6}$$

The magnetic term is for N interacting ions:

$$\mathcal{H}_2^B = \underbrace{B_0\sigma^0 \otimes S^z}_{R_2} + \underbrace{S^z \otimes B_0\sigma^0}_{L_2} \tag{7a}$$

$$\mathcal{H}_3^B = \underbrace{R_2 \otimes S^z}_{R_3} + \underbrace{S^z \otimes L_2}_{L_3} \tag{7b}$$

$$\vdots$$

$$\mathcal{H}_{N+1}^B = R_N \otimes S^z + S^z \otimes L_N \tag{7c}$$

where σ^0 is the identity in size 2×2 and $S^z = \sigma^z/2$ the spin operator in z.

2.4 Anisotropy term

Anisotropy is the property of a material to have different properties on depending on which symmetry axis the magnetic moment lies in. A material may have an axis on which a smaller magnetic field is necessary for magnetization, this is the easy axis, as opposed to an axis which requires the largest magnetic field for magnetization, the hard axis.

This property is described by the term

$$\mathcal{H}_{\text{anisotropy}} = -\sum_{ij} S_i^z I_{ij} S_j^z. \tag{8}$$

2.5 Spin-lattice coupling

The spin-lattice coupling is the relationship between the mechanical vibrations of a lattice and the magnetization due to the spin of ions localized at the lattice points. This coupling contributes to a number of phenomena in magnetic materials [10].

Phenomenologically, the origin of this coupling is the electron-phonon coupling and the interaction between electrons and the magnetic moments [11]. Phonons are quasiparticles which represent lattice vibrations and the electron-phonon coupling regards electron scattering of ions and phonon excitations, i.e. ionic vibrations. Itinerant, roaming, electrons then also interact with the magnetic moments of the ions. Thus, the electron mediates a coupling between the magnetic moments, spins, and the ion displacement, i.e. lattice vibrations. The electrons that mediate the coupling are part of the electronic background and this is an indirect exchange. See Figure 2.

The coupling is given by

$$\mathcal{H}_{\text{spin-lattice}} = -\sum_{ij} S_i^z \mathcal{A}_{ij} \cdot \langle \mathbf{Q}_j \rangle \tag{9}$$

where S_i^z are the spin operators in the z-direction, $\mathcal{A}_{ij}$ are the spin-lattice parameters, and $\langle \mathbf{Q}_j \rangle$ are the average displacement of ions in the lattice. The tensorial nature of the coupling is a result of previous research [11]. The variable $\langle \mathbf{Q}_j \rangle$, i.e. the average displacement is non-zero in the case of anharmonic oscillation of the

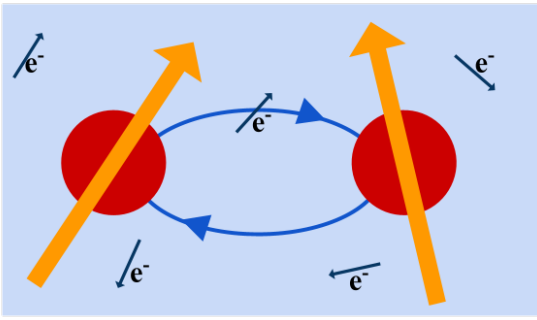

Figure 2: Electron exchange between ions in a metal.

lattice. For T = 0K this variable is zero, as well as for harmonic oscillation. The coupling is linear to the spin.

For a dimer, trimer and N chain system the spin-lattice Hamiltonian is given by:

$$\mathcal{H}_2^{\text{vib}} = S^z \otimes \alpha\sigma^0 + \alpha\sigma^0 \otimes S^z \tag{10a}$$

$$\mathcal{H}_3^{\text{vib}} = S^z \otimes \alpha\sigma^0 + \sigma^0 \otimes \mathcal{H}_2^{\text{vib}} \tag{10b}$$

$$\vdots$$

$$\mathcal{H}_{N+1}^{\text{vib}} = S^z \otimes \alpha\sigma^0 + \sigma^0 \otimes \mathcal{H}_N^{\text{vib}} \tag{10c}$$

where $\alpha = \sum_{ij} \mathcal{A}_{ij} \langle \mathbf{Q}_j \rangle$ and σ^0 the identity of relevant size. The parameter α is used extensively as the measure of vibration and lattice distortion and has the unit eV.

2.6 Model Hamiltonian

The model Hamiltonian for an atomistic finite spin chain with the Heisenberg term, Zeeman term, and the spin-lattice coupling then becomes

$$\mathcal{H} = -\sum_{i,j} (J_{i,j} \mathbf{S}_i \cdot \mathbf{S}_j + S_i^z I_{ij} S_j^z + S_i^z \mathcal{A}_{ij} \cdot \langle \mathbf{Q}_j \rangle) + B_0 \sum_i \mathbf{S}_i \tag{11}$$

where the exchange integral is only non-trivial for nearest neighbors in spin chain, i.e. J_{ij} is zero for non-consecutive i,j. Anisotropy is excluded from this study by setting I_{ij} to zero for all cases and is not considered further.

2.7 Net Magnetic Spin Moment

The magnetization of the system is the total magnetic moment of the system, i.e. how many spin up and down there are in the state which describes the system. The net magnetization of the system is understood by finding the probabilities of each state using statistical mechanics. For a closed system, such as the one studied in this report, the Gibbs distribution gives these probabilities:

$$p_{ij} = \frac{e^{-\varepsilon_i \beta}}{\sum_i e^{-\varepsilon_i \beta} \delta_{ij}} \tag{12}$$

where $\beta = 1/k_b T$ and ε_i are the energy eigenvalues. This means that the most probable state is the lowest energy state, the ground state. The magnetic moment is then given by

$$M = tr(xPx^\dagger Z) \tag{13}$$

where P is a matrix with diagonal elements p_{ij}, x are the eigenvectors, Z is the projection of the z direction spin operator on the chain. Z is found for an N length chain as:

$$Z_2 = S^z \otimes \sigma^0 + \sigma^0 \otimes S^z \tag{14a}$$
$$Z_3 = S^z \otimes \sigma^0 + \sigma^0 \otimes Z_2 \tag{14b}$$
$$\vdots$$
$$Z_{N+1} = S^z \otimes \sigma^0 + \sigma^0 \otimes Z_N \tag{14c}$$

3 Method

The model Hamiltonian, Eq. 11, is solved numerically for interacting chains of 2 – 10 spins. For the dimer and trimer systems, the eigenvalue problem is also solved analytically. Computing ability limits the chain size, since the Hamiltonian increases exponentially as $2^N \times 2^N$ where N is the number of interacting spins.

The eigenvalue problem is solved numerically in Matlab by first generating the Hamiltonian of the desired chain length though separate functions, then by applying the built-in function `eig()`. This returns the eigenvalues and eigenvectors. The magnetic moment of the system is then found using these results by finding the probability of each state through the Gibbs distribution, Eq.12. The sum of the probabilities are confirmed to be one. By varying parameters B_0 [eV] and α [eV], filled contour plots of the magnetic moment are generated. Other variable parameters are the exchange constant J [eV] and the temperature T [K].

The scripts necessary to generate the plots presented in this report are available in Appendix A and accompanying functions are in Appendix B.

A note can be made about the contour plots, i.e. phase diagrams, which make up the majority of the results. The diagrams show how regions of the same moment value form depending on B_0 and α. Due to the quantized nature of the chains, the moments are a multiple of $1/2$ and any other moment is a linear combination of different moment configurations. For example, the trimer has four possible pure moments ± 1.5 and ± 0.5. The value ± 1.5 is only possible for one state respectively, $|\uparrow\uparrow\uparrow\rangle$ and $|\downarrow\downarrow\downarrow\rangle$, while ± 0.5 is possible either as a single state or a linear combination of those with two up spins and one down and, respectively, one up spin and two down.

4 Results

In this section the dimer and trimer solutions are studied in detail and phase diagrams of the magnetic moment are presented for several finite spin chains. The exchange constant J is chosen to be negative, i.e. a antiferromagnetic coupling, and has the value -0.1 eV unless noted otherwise. The temperature is set to 3K in the Gibbs distribution and the resolution of the figures is 101×101 ($\alpha \times B_0$) unless noted otherwise.

4.1 Dimer

The dimer is the simplest case of the atomistic spin interactions since this has the minimal degrees of freedom with only two ions. This system is solved both analytically and numerically and thus forms a solid foundation upon which higher dimensional systems can be understood.

The Hamiltonian is

$$\mathcal{H} = -J\mathbf{S}_1 \cdot \mathbf{S}_2 - \sum_{ij} S_i^z \mathcal{A}_{ij} \cdot \langle \mathbf{Q}_j \rangle + B_0 \sum_i \mathbf{S}_i \tag{15a}$$

$$= \begin{pmatrix} -J/4 - \alpha + B_0 & 0 & 0 & 0 \\ 0 & J/4 & -J/2 & 0 \\ 0 & -J/2 & J/4 & 0 \\ 0 & 0 & 0 & -J/4 + \alpha - B_0 \end{pmatrix} \tag{15b}$$

where $\alpha = \sum_{ij} \mathcal{A}_{ij} \langle \mathbf{Q}_j \rangle$. This system has energies

$$-J/4 \mp \alpha \pm B, -J/4, 3J/4. \tag{16}$$

In the case of the parameter α vanishing, the solutions are a singlet state ($E_S = -3J/4, |S\rangle = 1/\sqrt{2}(|\uparrow\downarrow\rangle - |\downarrow\uparrow\rangle)$) with no degeneracy and a triplet state ($E_T = J/4, \{|-1\rangle = |\downarrow\downarrow\rangle, |1\rangle = |\uparrow\uparrow\rangle, |0\rangle = 1/\sqrt{2}(|\uparrow\downarrow\rangle + |\downarrow\uparrow\rangle)\}$) with a degeneracy of 3. The ground state is the triplet state for a ferromagnetic coupling (J > 0) and for an antiferromagnetic coupling (J < 0) it is the singlet state.

The energy spectrum for non-vanishing parameter α is presented in Figure 3a as well as the net magnetic moment. The existence of lattice vibrations break up the degeneracy of the energy spectrum. Here it is seen that for $|\alpha| > 0.1$ eV one of the triplet states, either $|-1\rangle$ or $|1\rangle$, becomes the ground state and the net magnetic moment is no longer zero, but -1 or 1. In Figure 3b, the net magnetic moment depending on both an applied field in the z-direction as well as α is presented.

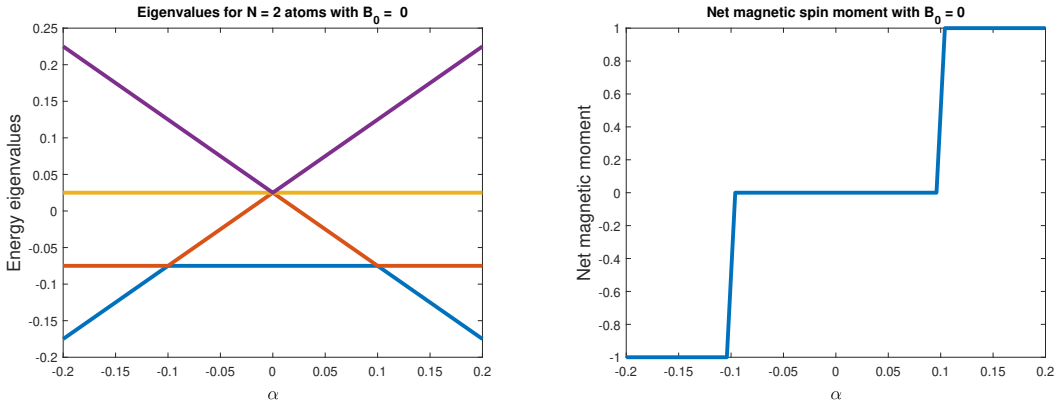

(a) (b)

Figure 3: The energy spectrum and net magnetic moment of a dimer with no applied B-field. In Figure 3a, the meeting point of purple, yellow and red is the triplet solution and blue is the singlet state. The singlet state is the ground state, until $|\alpha| > 0.1$ eV, after which one of the states $|\uparrow\uparrow\rangle$ or $|\downarrow\downarrow\rangle$ becomes the ground state. The color switch between blue and red is a result of the plotting, and the singlet state is constant at -0.75 eV. The switching of the ground state is also shown in Figure 3b, when the ground state magnetization becomes non-trivial for large enough $|\alpha|$.

4.2 Trimer

The trimer is the second system which is studied. This is the second smallest and is described by an 8×8 Hamiltonian. The net magnetic moment is presented in Figure 6a.

The basis for the trimer is

$$\begin{pmatrix} |\uparrow\uparrow\uparrow\rangle & |\uparrow\uparrow\downarrow\rangle & |\uparrow\downarrow\uparrow\rangle & |\uparrow\downarrow\downarrow\rangle & |\downarrow\uparrow\uparrow\rangle & |\downarrow\uparrow\downarrow\rangle & |\downarrow\downarrow\uparrow\rangle & |\downarrow\downarrow\downarrow\rangle \end{pmatrix}^T \tag{17}$$

where the first has magnetic moment +1.5, next two have +0.5, then one -0.5 and +0.5, then two -0.5 and lastly -1.5.

The region borders indicating phase transitions of the magnetic moment of the system is studied in more detail by setting $J = 0$ eV, see Figure 5. A trivial exchange constant results in a diagonal Hamiltonian and no linear combinations of states. The figure is similar to one with a non-zero J, see Figure 6a, but shifted along the B_0 axis.

The Hamiltonian of the trimer in matrix form is:

$$\mathcal{H}_3 = -\frac{1}{2}\begin{pmatrix} \frac{J}{2}-3\alpha+B_0 & 0 & 0 & 0 & 0 & 0 & 0 & 0 \\ 0 & -\alpha & \frac{J}{2} & 0 & 0 & 0 & 0 & 0 \\ 0 & \frac{J}{2} & -\frac{J}{2}-\alpha-B_0 & 0 & \frac{J}{2} & 0 & 0 & 0 \\ 0 & 0 & 0 & \alpha & 0 & \frac{J}{2} & 0 & 0 \\ 0 & 0 & \frac{J}{2} & 0 & -\alpha & 0 & 0 & 0 \\ 0 & 0 & 0 & \frac{J}{2} & 0 & -\frac{J}{2}+\alpha-B_0 & \frac{J}{2} & 0 \\ 0 & 0 & 0 & 0 & 0 & \frac{J}{2} & +\alpha & 0 \\ 0 & 0 & 0 & 0 & 0 & 0 & 0 & -\frac{J}{2}+3\alpha+B_0 \end{pmatrix}. \tag{18}$$

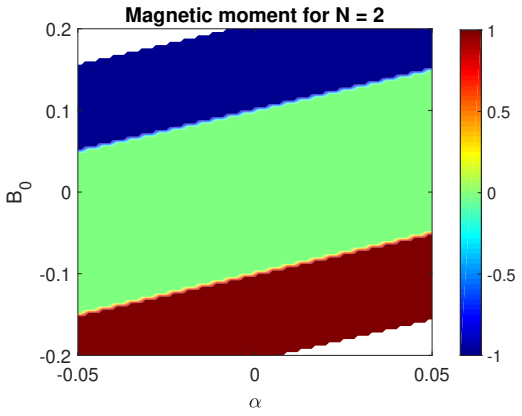

Figure 4: Net magnetic moment for dimer with varying B-field and α. This shows the same results as Figure 3b but with a varying B_0 and smaller α-axis. The white region are NaN values. The jagged transitions between the regions are due to artefacts in the plotting.

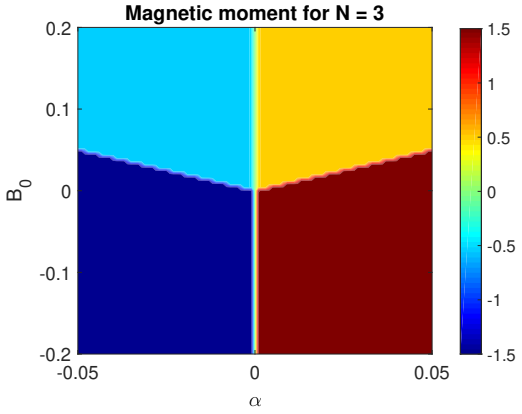

Figure 5: Net magnetic moment of trimer with J = 0 eV.

By setting the exchange constant $J = 0$ eV, the Hamiltonian is diagonal and the eigenvalues are

$$\frac{1}{2}\begin{pmatrix} -3\alpha + B_0 \\ -\alpha \\ -\alpha - B_0 \\ \alpha \\ -\alpha \\ \alpha - B_0 \\ \alpha \\ 3\alpha + B_0 \end{pmatrix}. \tag{19}$$

These eigenvalues can be used to describe the phase transitions. For negative α, two states can take the minimum, ground state, eigenvalue: $\alpha - B_0$ with $|\downarrow\uparrow\downarrow\rangle$ when $\alpha > -B_0$ and $3\alpha + B_0$ with $|\downarrow\downarrow\downarrow\rangle$ when $\alpha < -B_0$. Then for positive α values there are also two states which can take the most negative value: $|\uparrow\uparrow\uparrow\rangle$ for $\alpha > -B_0$ and $|\uparrow\downarrow\uparrow\rangle$ when $\alpha < -B_0$.

4.3 Longer spin chains

The phase diagrams of the net magnetic moment is also found for larger systems of 3 to 10 interacting spins in a linear chain, see Figures 6 and 7. The resolution is decreased for calculations of Figure 7b since this is a very large calculation. White spaces in Figure 7 are caused by NaN values, since the Gibbs distribution term becomes too large for the computer to calculate.

The figures are all colored according to their possible highest and lowest magnetic moment configuration, with dark red for N/2 and dark blue for -N/2. The spin-lattice coupling parameter α runs between -0.5J and +0.5J and the magnetic field B_0 between -2J and 2J.

The phase diagrams show a behavior of convergence to a common phase diagram for longer spin chains. Compare in particular Figures 7a and 7b, with N = 9 and N = 10. These two figures are quite similar to each other with the moment regions having similar positions and the phase transitions between them straightening out. It should be noted that the resolution of N = 10 is lower. As the spin chain becomes longer, more moment regions are present and the phase transition divisions between regions appear to become constant values of α. Symmetry is also exhibited in all systems.

In both odd and even systems, the number of regions with positive versus negative moments are equal. For odd numbered chains, there are (N+1)/2 positive/negative moment regions, and for even numbered there are N/2. So both the trimer and N = 4 system have two positive moment regions and two negative.

In all systems, the observation can be made that for $\alpha < 0$ the net magnetic moment is generally negative and for $\alpha > 0$ the net magnetic moment is generally positive. There are exceptions to this in the even numbered chain, for example the orange and light blue regions of Figure 6b exist for both positive and negative α. The coupling parameter α acts effectively as a magnetic field.

In the phase diagrams of odd numbered chains, Figures 6a, 6c, 6e, and 7a, there are common features. There is a clear phase transition at $\alpha = 0$ for all values of B_0, this is also a symmetry line over which the plot is mirrored in the opposite sign according to the sign of α. The lowest and highest magnetic moment (dark blue and dark red) always occur with a negative external magnetic field. The moments closest to zero (± 0.5) occur always adjacent to $\alpha = 0$ line and flip every other odd chain of being in the top half of the figure and bottom half, compare Figures 6c and 6e. This corresponds to whether the number of positive/negative regions (N+1)/2 is even or odd.

The even numbered spin chains also have common features, see Figures 4, 6b, 6d, 6f, and 7b. These Figures show mirroring symmetry over some diagonal. Here the lowest magnetic moments (dark blue) occur at positive external magnetic fields and the highest (dark red) at negative. There is diagonal flipping of the systems, the green unmagnetized regions exist in quadrants I and III and quadrants II and IV, every other even chain. For example compare Figures 4, 6b, 6d. There is symmetry over some diagonal line in quadrants I and III when the number of positive/negative moment regions (N/2) is odd (example N = 6, Figure 6d), and quadrants II and IV when this number is even (example N = 4, Figure 6b).

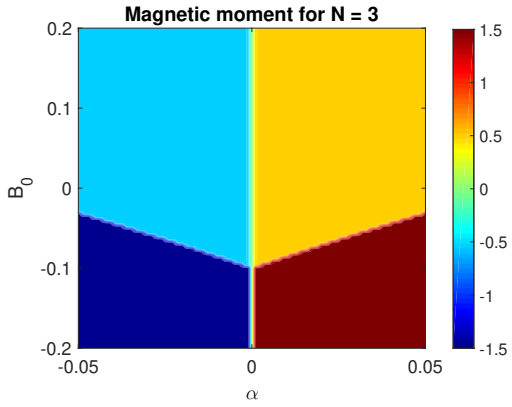

(a) N = 3. Yellow (+0.5), light blue (-0.5), dark blue (-1.5), dark red (+1.5).

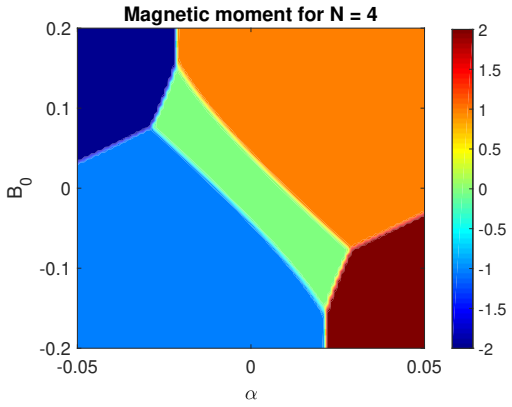

(b) N = 4. Green (0), orange (+1), dark blue (-2), light blue (-1), dark red (+2).

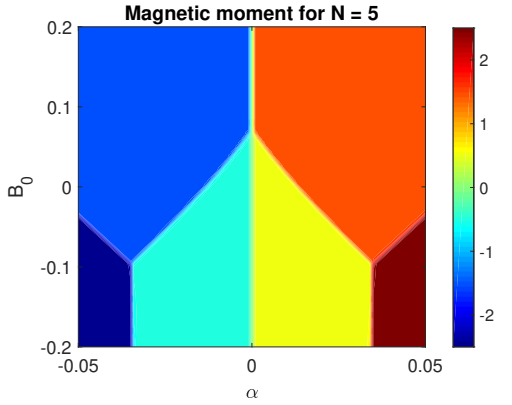

(c) N = 5. Yellow (+0.5), orange (+1.5), dark red (+2.5), light blue (-0.5), blue (-1.5), dark blue (-2.5).

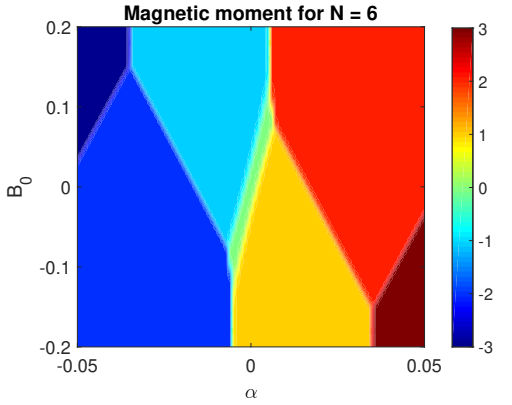

(d) N = 6. Green (0), yellow (+1), red (+2), dark red (+3), light blue (-1), blue (-2), dark blue (-3).

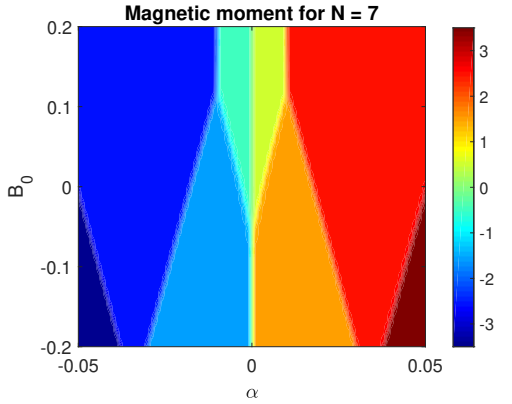

(e) N = 7.

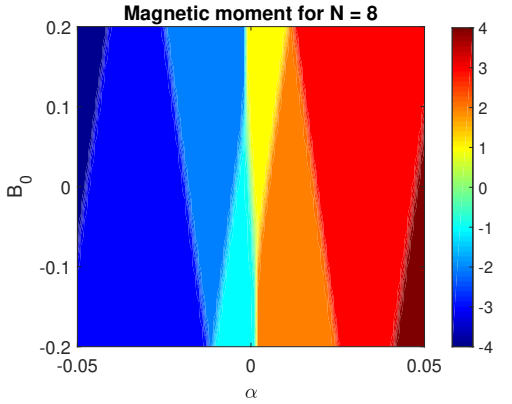

(f) N = 8.

Figure 6: Net magnetic moments of systems with 3-8 interacting spins.

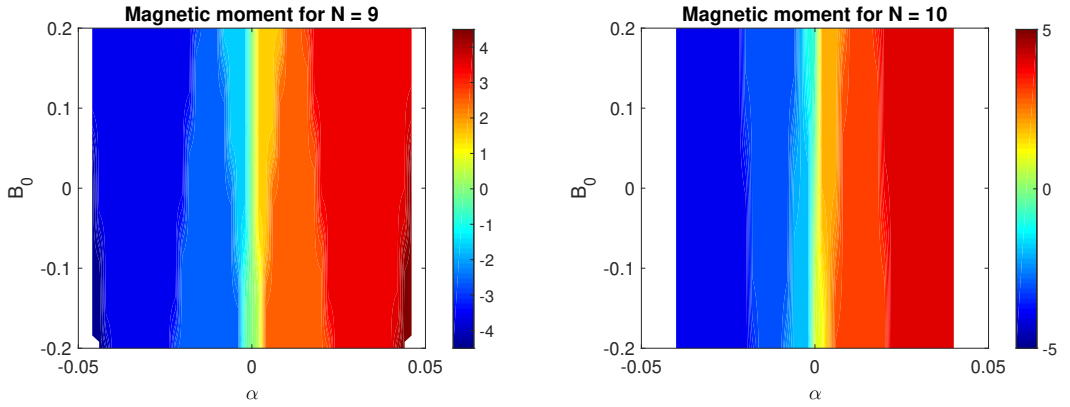

(a) N = 9. (b) N = 10.

Figure 7: Net magnetic moments of systems with 9 and 10 interacting spins. For both figures, the diagram is of lower resolution than others, with a grid of 51x51.

4.4 Temperature dependence

The net magnetic moment of systems with different temperature in the Gibbs distribution are also calculated. In Figure 8, the net magnetic moment for a dimer at 30K and 300K is presented. Here it is clearly seen that at higher temperatures the separation between states is smeared out compared to Figure 4 where the division between regions is distinct. This temperature dependence is also shown in the case of the trimer and quadmer systems, presented in Figure 9 and 10 respectively.

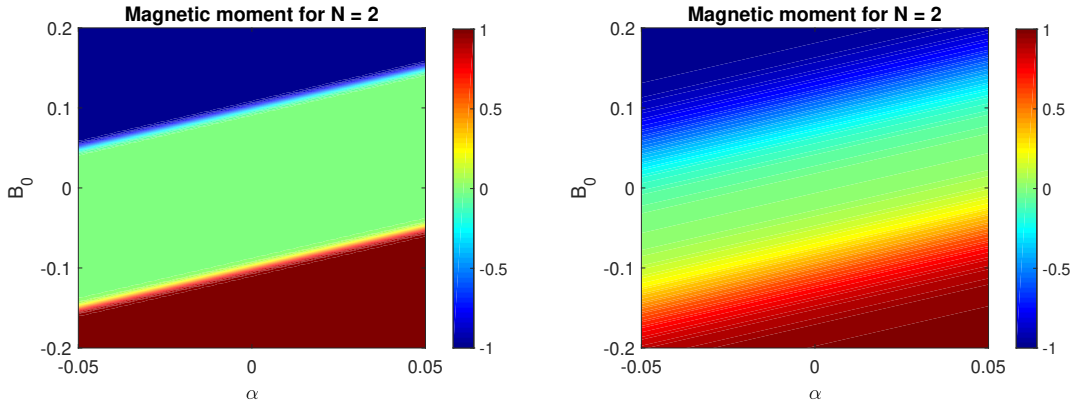

(a) T = 30K (b) T = 300K

Figure 8: Temperature dependence of the net magnetic moment of a dimer.

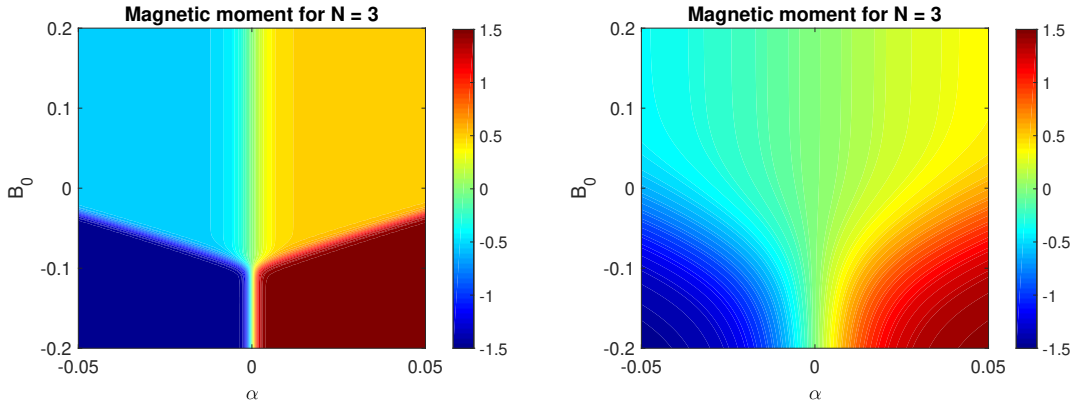

(a) T = 30K (b) T = 300K

Figure 9: Temperature dependence of the net magnetic moment of a system of 3 interacting spins.

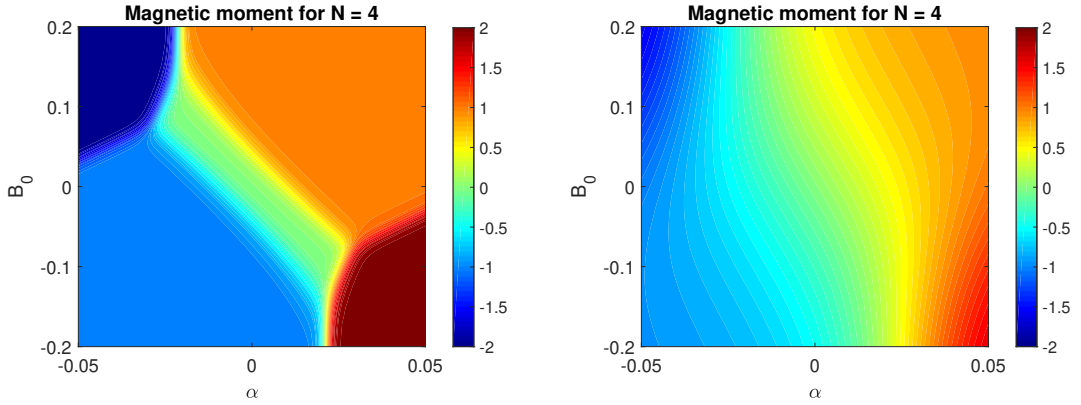

(a) T = 30K (b) T = 300K

Figure 10: Temperature dependence of the net magnetic moment of a system of 4 interacting spins.

5 Discussion

The purpose of this project is to observe the dependence of the spin-lattice coupling on a finite spin chain. Figures 6 and 7 present pictures of the effect of the spin-lattice coupling parameter α. The features of these phase diagrams show that they seemingly converge to a common phase diagram for larger spin chains and positive moment regions exist for positive α and negative for negative α with no clear dependence on the sign of the external magnetic field.

Convergence of the phase diagrams as the spin chains are longer implies that an analytic model of the spin-lattice coupling behavior can perhaps be found through future studies. The results presented here, suggest that the moment regions will become a gradient, the absolute moment value increasing with $|\alpha|$ and the phase transitions between regions will possibly exist at constant values of α.

The feature that for positive α the magnetic moment is positive and for negative α the moment is negative suggests the proposition that the spin-lattice coupling parameter α acts as a magnetic field on the system and may be much stronger than an applied external field.

Another feature that corroborates this hypothesis, is how in the even chains the most negative moment region exists where the z-direction of the applied magnetic field is positive and thus oppositely aligned. Likewise, in both the even and odd chains, the most positive moment region appears when the applied field is aligned in the negative z-direction, oppositely to the state.

The 30K and 300K phase diagrams of the moments of chain length 3 and 4, Figures 9 and 10, show that the effects of α are present at higher temperatures, such as room temperature. Larger temperatures result in smearing out of the region divisions. This may imply that lattice vibrations could be a reason for the temperature activated ferromagnetism recently discovered in certain materials by Dhara, et.al. (2016) [4] and Mondal, et.al. (2020) [5].

In an experimental setting this study could be used to predict results and therefore it is important to look at realistic values of the parameters used. The parameter α is the basis of this study. It describes the size of the coupling. Realistic values of the parameter are smaller than what is presented in the theoretical calculations, and should more reasonably be on the order of $J/10$. Relevant values of J are on the order of meV to eV; in this study J = -0.1 eV is used. Further, is the question whether α may be negative which does not have an answer as of yet, but for the purpose of being general this possibility is included in this study.

Another parameter value that needs to be discussed is B_0 which describes the external applied magnetic field. Since this is a theoretical work, this parameters minimum and maximum values are much larger than what would be used in any physical experiment, since $B_0 = 0.1$ eV ≈ 950 T. These large values are included since they can be and to give a broader picture of the effect of the coupling.

This theoretical study presents a framework on which both future theoretical and experimental work can be based. The strengths of this being a theoretical study are that the results give a wider picture of the effect of the spin-lattice coupling on a finite spin chain due to the flexibility of the calculations made. The results present phase diagrams of the moment of the system for up to chains of length 10; this means that observations of systemic changes can be discussed, such as an apparent convergence.

However, the study has some limitations as well. With more efficient coding and larger computation capacity, larger spin chain systems could be observed. The work is also limited to the nearest neighbor approximation for the Heisenberg model as well as a one-dimensional lattice. The model is a bi-linear model and thus also limited to pairwise interactions. Further, there are many results presented for which no physical explanation is given. One goal with this work was to systematically describe the effect of the coupling and this is not fulfilled in its entirety, rather observations are made of the features of the effects and some speculations are made. This study presents many unanswered questions about the spin-lattice coupling and its effect on spin chains. Future studies on the current topic are therefore recommended.

There are many ways of continuing this work. Improving coding efficiency and computing capacity would lead to phase diagrams of larger systems which could show the convergence more clearly. While this would provide more ground to make observations on the systemic effects of the lattice vibrations, more importantly, more work is necessary to describe the physical effects and find analytical descriptions of the coupling. Due to this work being limited to one-dimensional systems of interacting spins, it would also be prudent to present the same results for two- and three-dimensional lattice configurations. It might also be relevant to study internal magnetic field effects.

6 Conclusion

The magnetic moments of finite spin chains of different lengths with a spin-lattice coupling and applied external magnetic field are presented. These constitute a systematic observation of the effects of the spin-lattice coupling. The phase diagrams present features such as a large dependence on the sign and size of the lattice vibration coupling parameter α and an indication that the effects converge for larger chain systems. Two propositions are made on the basis of these features: that the effects of α converge to a common phase diagram for long spin chains and that the effects of the coupling is stronger than external magnetic field effects. High temperature behaviour is also presented, and shows that the spin-lattice coupling is relevant at room temperature. Further studies must be made on the coupling to understand the behavior and an analytical model be made.

7 Bibliography

[1] Atsufumi Hirohata, Keisuke Yamada, Yoshinobu Nakatani, Ioan-Lucian Prejbeanu, Bernard Diény, Philipp Pirro, and Burkard Hillebrands. Review on spintronics: Principles and device applications. *Journal of magnetism and magnetic materials*, 509:166711, 2020.

[2] N. A. Spaldin and R. Ramesh. Advances in magnetoelectric multiferroics. *Nature materials*, 18(3):203–212, 2019.

[3] Blai Casals, Nahuel Statuto, Michael Foerster, Alberto Hernández-Mínguez, Rafael Cichelero, Peter Manshausen, Ania Mandziak, Lucía Aballe, Joan M. Hernàndez, and Ferran Macià. Generation and imaging of magnetoacoustic waves over millimeter distances. *Physical review letters*, 124(13):137202–137202, 2020.

[4] Barun Dhara, Kartick Tarafder, Plawan K. Jha, Soumendra N. Panja, Sunil Nair, Peter M. Oppeneer, and Nirmalya Ballav. Possible room-temperature ferromagnetism in self-assembled ensembles of paramagnetic and diamagnetic molecular semiconductors. *The journal of physical chemistry letters*, 7(24):4988–4995, 2016.

[5] Amit K. Mondal, Noam Brown, Suryakant Mishra, Pandeeswar Makam, Dahvyd Wing, Sharon Gilead, Yarden Wiesenfeld, Gregory Leitus, Linda J. W. Shimon, Raanan Carmieli, David Ehre, Grzegorz Kamieniarz, Jonas Fransson, Oded Hod, Leeor Kronik, Ehud Gazit, and Ron Naaman. Long-range spin-selective transport in chiral metal–organic crystals with temperature-activated magnetization. *ACS nano*, 14(12):16624–16633, 2020.

[6] Charles Kittel and Paul McEuen. *Introduction to solid state physics*. Wiley, Hoboken, N.J, 8. edition, 2005.

[7] Olle Eriksson, Anders Bergman, Lars Bergqvist, and Johan Hellsvik. *Atomistic spin dynamics: foundations and applications*. Oxford University Press, Oxford, 2017.

[8] Wolfgang Nolting and Anupuru Ramakanth. *Quantum theory of magnetism*. Springer, Heidelberg;New York;, 2009;2008;.

[9] H. Ibach and H. Lüth. *Solid-state physics: an introduction to principles of materials science*. Springer, New York, Berlin, 4 edition, 2009, 2010.

[10] Shuai Dong, Jun-Ming Liu, Sang-Wook Cheong, and Zhifeng Ren. Multiferroic materials and magnetoelectric physics: symmetry, entanglement, excitation, and topology. *Advances in physics*, 64(5-6):519–626, 2015.

[11] J. Fransson, D. Thonig, P. F. Bessarab, S. Bhattacharjee, J. Hellsvik, and L. Nordström. Microscopic theory for coupled atomistic magnetization and lattice dynamics. *Physical review materials*, 1(7), 2017.

A Main scripts

A.1 NSpinsystem_alphaVarying.m

```
%finding energy spectrum for N spin system with
   Heisenberg model for exchange interaction (S),
   lattice vibration (vib) and magnetic field (B) and
   net magnetic spin moment (moment) is also found


% parameters
N = 2; % minimum N = 2
J = -0.1; %[eV] exchange coupling constant
B0 = 0.000; % [eV] magnetic field
alpha = linspace(-2*abs(J),2*abs(J),101); %[eV]
T = 3; %[K]

% constants
kb = 8.617342E-5; %[eV/K] Boltzmanns constant
beta = 1/(kb*T);
SSz = SpinMatrix(N);

% Hamiltonian
[S, f] = HeisenbergTerm(N); % f is the factor (1/2)^N
B = MagneticTerm(B0, N);

lenAlpha = length(alpha);
eigvec = zeros(2^N,2^N,lenAlpha);
eigval = zeros(2^N,2^N,lenAlpha);

for idx = 1:lenAlpha %vary alpha
    vib = VibrationTerm(alpha(idx), N); %lattice part of
        hamiltonian

    H = -J*f*S-vib+B; %hamiltonian
    [eigvec(:,:,idx), eigval(:,:,idx)] = eig(H); %
       eigenvectors and eigenvalues
end

% reshaping eigenvalue matrix (4x4xlenAlpha) into matrix
    lenAlpha x 4 with eigenvectors in columns for
   plotting
ev = zeros(lenAlpha, 2^N);
figure(1)
clf
for idx = 1:2^N
```

```
36      ev(:,idx) = reshape(eigval(idx,idx,:), [lenAlpha,1])
            ;
37
38      plot(alpha, ev(:,idx), '-', 'Linewidth', 3)
39      hold on
40  end
41
42  hold off
43  title(['Eigenvalues for N = ', num2str(N), ' atoms with
        B_0 =  ', num2str(B0)])
44  xlabel('\alpha', 'FontSize', 14)
45  ylabel('Energy eigenvalues', 'FontSize', 14)
46
47
48  % calculating and plotting net magnetic spin moment
49
50  Gdist = zeros(2^N,2^N);
51  prob = zeros(lenAlpha,1);
52  moment = zeros(lenAlpha,1);
53  for idx = 1:lenAlpha
54      x = diag(eigval(:,:,idx)); % eigenvalues in column
            vector
55      xx = eigvec(:,:,idx);
56      Gdist(:,:) = diag(exp(-x*beta))/sum(exp(-x*beta)); %
            Gibbs distribution
57      prob(idx) = trace(Gdist(:,:));
58      moment(idx) = trace(real(xx*Gdist*xx')*SSz);
59  end
60
61  figure(2)
62  clf
63  plot(alpha, moment, 'Linewidth', 3)
64  title(['Net magnetic spin moment with B_0 = ', num2str(
        B0)])
65  xlabel('\alpha', 'FontSize', 14)
66  ylabel('Net magnetic moment', 'FontSize', 14)
67  set(gcf,'units','centimeters','position',[0 0 16 14])
68  yticks([-1 -0.5 0 0.5 1])
69  xticks([-0.2 -0.1 0 0.1 0.2])
70  set(gca, 'FontSize', 14)
```

A.2 Phasediagrams_NSpinSystem.m

```
% finding magnetic moments of finite spin systems of N interacting spins with varying spin-lattice coupling parameter alpha and external magnetic field B0

% parameters
N = 2;
J = -0.1;
I = -J/1000; % anisotropy
alpha = linspace(-0.5*abs(J),0.5*abs(J),101);
B0 = linspace(-2*abs(J), 2*abs(J),101);
T = 3; %[K]

% constants for magnetic moment calculation
kb = 8.617342E-5; %[eV/K] Boltzmanns constant
beta = 1/(kb*T);
SSz = SpinMatrix(N);

% Hamiltonian terms
[S, f] = HeisenbergTerm(N); %Heisenberg model, f is the factor (1/2)^N
anis = AnisotropyTerm(I,N);

lenAlpha = length(alpha);
lenB0 = length(B0);
moment = zeros(lenAlpha,lenB0);

for bidx = 1:lenB0 % vary B0
    B = MagneticTerm(B0(bidx), N);

    for aidx = 1:lenAlpha %vary alpha
        vib = VibrationTerm(alpha(aidx), N); %lattice part of hamiltonian

        H = -J*f*S-vib+B; %hamiltonian
        [eigvec, eigval] = eig(H);

        x = diag(eigval); % eigenvalues in column vector
        xx = eigvec;
        Gdist = diag(exp(-x*beta))/sum(exp(-x*beta)); % Gibbs distribution
        moment(aidx,bidx) = trace(real(xx*Gdist*xx')*SSz);
    end
end
```

```
39
40 % plotting %%%%%%%%%%%%%%%%%%%
41 figure(1)
42 clf
43 contourf(alpha, B0, moment', 100, 'LineStyle', 'none')
44 caxis([-N/2,N/2])
45 colormap jet
46 colorbar
47 %title(['Net magnetic moment for N = ', num2str(N),'
      interacting spins'], 'FontSize', 11)
48 title(['Magnetic moment for N = ', num2str(N), ' and T =
      ', num2str(T), ' K'], 'FontSize', 16)
49 xlabel('\alpha', 'FontSize', 20)
50 ylabel('B_0', 'FontSize', 16)
51 yticks([-0.2 -0.1 0 0.1 0.2])
52 xticks([-0.05 0 0.05])
53 %set(gcf,'units','centimeters','position',[0 0 16 14])
54 set(gca, 'FontSize', 14)
```

B Functions

B.1 HeisenbergTerm.m

```
function [H, factor] = HeisenbergTerm(N)
% function [H, factor] = HeisenbergTerm(N)
% function to find the spin-operator tensor product for
   any number of interacting spins (N)

% pauli matrices
sx = [0 1; 1 0];
sy = [0 -1i; 1i 0];
sz = [1 0; 0 -1];

Sx = kron(sx,sx);
Sy = kron(sy,sy);
Sz = kron(sz,sz);

S = Sx + Sy + Sz;

idx = 2;
while idx < N
    S = kron(S,eye(2)) + kron(eye(2),S);
    idx = idx + 1;
end

H = S;
factor = (1/2)^N;
```

B.2 VibrationTerm.m

```
function [vib] = VibrationTerm(alpha, N)
% function [vib] = VibrationTerm(alpha, N)
% function to generate vibration matrix (alpha matrix)
   for N interacting spins with coupling alpha

sz = 1/2*[1 0; 0 -1]; %pauli in z
Id = eye(2); % identity

right = kron(sz, alpha.*Id);
left = kron(alpha.*Id, sz);

idx = 2;
while idx < N
    vib = right + left;
```

```
    right = kron(sz, alpha.*eye(2^idx));
    left = kron(eye(2), vib);
    idx = idx + 1;
end

vib = right + left; %lattice vibration part of
   hamiltonian
```

B.3 MagneticTerm.m

```
function [B] = MagneticTerm(B0, N)
% function [B] = MagneticTerm(B0, N)
% function to generate magnetic field term in
   Hamiltonian with strength B0 for N interacting spins

s = 1/2*[1 0; 0 -1]; %sz pauli matrix
Id = eye(2); % identity

right = kron(s, B0.*Id);
left = kron(B0.*Id, s);

idx = 2;
while idx < N
    right = kron(s, right);
    left = kron(left, s);
    idx = idx + 1;
end

B = right + left; %magnetic part of Hamiltonian
```

B.4 AnisotropyTerm.m

```
function [ani] = AnisotropyTerm(I, N)
% function [ani] = AnisotropyTerm(I, N)
% function to generate anisotropy term in Hamiltonian
   with strength I for N interacting spins

sz = 1/2*[1 0; 0 -1]; %pauli in z
sz2 = sz^2;
Id = eye(2); % identity

right = kron(sz2, I.*Id);
left = kron(I.*Id, sz2);

```

```
idx = 2;
while idx < N
    ani = right + left;
    right = kron(sz2, I.*eye(2^idx));
    left = kron(I.*eye(2), ani);
    idx = idx + 1;
end

ani = right + left; %anisotropy part of Hamiltonian
```

B.5 SpinMatrix.m

```
function [SS] = SpinMatrix(N)
% function [SS] = SpinMatrix(N)
% function to create the spin matrix for finding net
   magnetic moment of system with N interacting atoms in
    z direction

s0 = eye(2);
s = [1 0; 0 -1]/2; %sz

S1 = kron(s,s0);
S2 = kron(s0,s);
SS = S1+S2;

idx = 2;
while idx < N
    SS = kron(s0, SS) + kron(s, eye(2^idx));
    idx = idx + 1;
end
```